Research Article

Rapid Communications in Mass Spectrometry

Received: 6 August 2016 Revised: 27 November 2016 Accepted: 28 November 2016 Published online in Wiley Online Library

Rapid Commun. Mass Spectrom. **2017**, *31*, 381–388
(wileyonlinelibrary.com) DOI: 10.1002/rcm.7801

Depth profiling cross-linked poly(methyl methacrylate) films: a time-of-flight secondary ion mass spectrometry approach

Soheila Naderi-Gohar[1,2†], Kevin M.H. Huang[1‡], Yiliang Wu[3¶], Woon Ming Lau[4] and Heng-Yong Nie[1,2*]

[1]Surface Science Western, The University of Western Ontario, 999 Collip Circle, London, Ontario N6G 0J3, Canada
[2]Department of Physics and Astronomy, The University of Western Ontario, London, Ontario N6A 3K7, Canada
[3]Advanced Materials Laboratory, Xerox Research Centre of Canada, Mississauga, Ontario L5K 2L1, Canada
[4]Chengdu Green Energy and Green Manufacturing Technology R&D Center, Chengdu, Sichuan 610207, China

RATIONALE: In order to determine the degree of cross-linking on the surface and its variations in a nanometer-scale depth of organic materials, we developed an approach based on time-of-flight secondary ion mass spectrometry (TOF-SIMS), which provides rich chemical information in the form of fragment ions. TOF-SIMS is extremely surface-sensitive and capable of depth profiling with the use of a sputter ion beam to remove controllable amounts of substance.
METHODS: Poly(methyl methacrylate) (PMMA) films spin-coated on a Si substrate were cross-linked using a recently developed, surface sensitive, hyperthermal hydrogen projectile bombardment technique. The ion intensity ratio between two ubiquitous hydrocarbon ions, C_6H^- and C_4H^-, detected in TOF-SIMS, denoted as ρ, was used to assess the degree of cross-linking of the PMMA films. The cross-linking depth of the PMMA films was revealed by depth profiling ρ into the polymer films using a C_{60}^+ sputter beam.
RESULTS: The control PMMA film spin-coated on a Si substrate was characterized by ρ = 32% on its surface when using a 25 keV Bi_3^+ primary ion beam. This parameter on the PMMA films subjected to HHIC treatment for 10, 100 and 500 s increased to 45%, 56% and 65%, respectively. The depth profiles of ρ obtained using a 10 keV C_{60}^+ ion beam resembled an exponential decay, from which the cross-linking depth was estimated to be 3, 15 and 39 nm, respectively, for the three cross-linked PMMA films.
CONCLUSIONS: We demonstrated that the ion intensity ratio of C_6H^- to C_4H^- detected in TOF-SIMS provides a unique and simple means to assess the degree of cross-linking of the surface of PMMA films cross-linked by the surface sensitive hyperthermal hydrogen projectile bombardment technique. With a C_{60}^+ sputter beam, we were able to depth profile the PMMA films and determine cross-linking depths of the cross-linked polymer films at nanometer resolutions. Copyright © 2016 John Wiley & Sons, Ltd.

Spin coating thin polymer films onto a substrate is a simple approach to achieve functionalized surfaces for applications in photoresists and anti-bacterial surfaces, as well as biological sensors.[1–6] More recently, development of organic semiconductors has led to a new industry of organic electronics, where functional polymer films including semiconductors and dielectrics are usually solution-processed on a substrate.[7–12] In order to achieve appropriate chemical stability and mechanical strength for such solution-processed polymer films, their molecules need to be cross-linked. Conventional cross-linking approaches rely on the incorporation of cross-linking agents into the solutions in which both the polymer and the cross-linking agent are dissolved.[13–15] These approaches require additional chemicals, as well as heating or irradiation, to complete the cross-linking (curing) process, which may affect the functionality of the spin-coated polymer films.

Recently, hyperthermal hydrogen projectiles have been demonstrated to be able to cross-link hydrocarbon chains in molecular or polymeric films.[16] In this method, which is described as hyperthermal hydrogen induced cross-linking (HHIC), energetic H_2 projectiles impact the surface of a polymer film and preferentially knock out the hydrogen atoms from the C–H bonds of hydrocarbon chains, resulting in carbon radicals and leading to the formation of C–C bonds between adjacent hydrocarbon chains. The HHIC technique requires only a small amount of H_2, thus eliminating additional chemicals such as cross-linking agents. It is rapidly becoming a cross-linking technique in the surface engineering of inert substrates with grafted and cross-linked polymeric films, having advantages such as antibacterial surfaces, protein- and cell-resistant surfaces.[4,5,17]

* *Correspondence to:* H.-Y. Nie, Surface Science Western, The University of Western Ontario, 999 Collip Circle, London, Ontario N6G 0J3, Canada.
E-mail: hnie@uwo.ca

† Present address: Advanced Mineral Technology Laboratory, 100 Collip Circle, London, Ontario N6G 4X8, Canada

‡ Present address: Amec Foster-Wheeler, 700 University Avenue, Toronto, Ontario M5G 1X6, Canada

¶ Present address: TE Connectivity, 306 Constitution Drive, Menlo Park, CA 94025, USA

For a cross-linked polymer film, it is important to be able to assess its degree and depth of cross-linking. In previous studies, the cross-linking in polymer films by the HHIC technique was demonstrated by enhanced resistance to solvent attack and an increased Young's modulus.[16,18] The depth and degree of a cross-linked polymer film are important in understanding the cross-linked portion of the polymer film subjected to HHIC treatment. In general, many of the conventional methods used to investigate degrees of cross-linking of a polymer film involve looking at the amount of dissolved portion of the polymer,[19] which is perhaps unsuitable for materials where only the top several nanometers are cross-linked. There is thus an urgent need to develop a surface-sensitive technique to probe the degree and depth of cross-linked polymer films by HHIC. Therefore, we have investigated the development of an analytical methodology using time-of-flight secondary ion mass spectrometry (TOF-SIMS),[20] which is especially powerful in revealing chemical information from a surface.[13–17] In this technique, a pulsed (primary) ion beam is used to bombard the surface of a specimen to generate (secondary) ions from the topmost monolayers (1–3 nm). The secondary ions are extracted, mass-separated and detected in parallel, providing a powerful approach to understanding surface chemistry. Among the various surface analytical techniques that yield information about elemental and molecular species, TOF-SIMS is a surface-sensitive approach for detecting fragment ions characteristic of organic molecules with high mass resolution.[21–25] With another ion beam serving to sputter a controllable amount of substance from the surface, chemical variations in the depth direction can also be accessed. It has been demonstrated that C_{60}^+, a cluster ion beam, can be used to depth-profile some types of organic molecular layers and polymers.[26–30]

TOF-SIMS provides extremely rich chemical information; that is, all the ions generated are captured, leading to the possibility of identifying chemicals and exploring surface chemistry. Extracting such information to identify chemicals and explore their effect on surface chemistry is commonly referred to as data mining. For example, even the ubiquitous hydrocarbon ions can be used to explore the chemical structures of polymers.[31–34] By analyzing the ion intensities of $C_{2n}H^-$ ions from polyethylene (PE), polypropylene (PP), polyisoprene (PIP) and polystyrene (PS), which have different chemical structures in terms of carbon "densities" (i.e., C/H ratios), one of the authors showed that intrinsic relationships existed among $C_{2n}H^-$ ions.[34] Specifically, it was found that the ion intensity ratio between C_6H^- and C_4H^- is a useful parameter, serving to quantitatively differentiate the chemical structures of the four polymers.[34] Because the cross-linking of polymer films using the HHIC technique is basically a process of reduction of hydrogen atoms, or increase in carbon "density", we demonstrate the feasibility of using the intensity ratio between the ubiquitous hydrocarbon species C_6H^- and C_4H^- to quantify the degrees of cross-linking, as well as their variations into spin-coated polymer films. We selected poly(methyl methacrylate) (PMMA) as a model system for our HHIC experiment and TOF-SIMS investigation. In polymeric composite areas, PMMA has been widely used as the matrix for making carbon nanotube composites.[35] More recently, PMMA has been identified as a key substance for organic dielectrics used in organic electronic devices.[36,37] The development of this TOF-SIMS approach to quantify the degree and depth of cross-linking of organic molecules is expected to promote applications of TOF-SIMS in the chemical analysis of cross-linked polymer films.

EXPERIMENTAL

The PMMA (M_w = 97000, M_n = 44700) used in this study was purchased from Sigma-Aldrich (St. Louis, MO, USA). PMMA films were spin-coated at a spin rate of 4000 rpm onto silicon substrates using a 5 wt.% PMMA solution in chloroform. The film thickness was approximately 200 nm as determined using a KLA Tencor P-10 stylus profilometer (Milpitas, CA, USA) with a diamond probe having a radius of 2 μm. Four PMMA film samples were prepared, three of which were subjected to HHIC treatment for 10, 100 and 500 s.

The details of the HHIC technique have been reported elsewhere;[16] only the experimental conditions are described herein. The HHIC experiment was carried out using a home-made reactor[16] having a sample chamber with a base pressure of 2×10^{-6} Torr and a plasma generating system consisting of a microwave source and an electron cyclotron resonance (ECR) unit (Applied Science and Technology, Inc., Woburn, MA, USA). The microwave frequency was 2.45 GHz, requiring an applied magnetic field strength of 87.5 mT. Protons generated by the ECR microwave plasma in the ECR unit fed with H_2 were extracted with a potential energy of –100 eV and directed to the drift zone (50 cm in length) which was fed with another H_2 inlet, reaching a pressure of 2×10^{-3} Torr. Inside the drift zone, a cascade of collisions between the energetic protons extracted from the plasma and H_2 molecules produced energetic H_2 projectiles heading downstream. In front of the sample stage there were two metallic grids having potential differences of 100 and –50 V to deflect positively and negatively charged particles, respectively, so that only neutral H_2 projectiles (with a kinetic energy 5–20 eV) arrived at the samples placed at the bottom in the drift zone. When these H_2 projectiles collided with the surface of an organic film, its C–H bonds were cleaved preferentially due to the kinematic selectivity of energy transfer from the energetic H_2 projectiles to hydrogen atoms in the organic molecules.[16] The induced cross-linking reactions produced a molecular layer having a controllable degree of cross-linking, while retaining the desirable chemical functionalities of the organic molecules. Upon HHIC treatment, a stream of nitrogen gas was flooded into the chamber to vent the reactor.

A TOF-SIMS IV instrument (ION-TOF GmbH, Münster, Germany) equipped with a cluster bismuth liquid metal ion gun was employed to investigate the surface chemistry of PMMA films cross-linked using the HHIC technique. The base pressure of the TOF-SIMS analytical chamber was about 7.5×10^{-9} Torr. A pulse of 25 keV Bi_3^+ cluster primary ion beam (with a pulse width of ~ 1 ns and a target current of ~1 pA) was used to bombard the sample to generate secondary ions. The secondary ions were extracted using an extraction voltage of 2 kV, mass-separated, and detected via a reflectron type of time-of-flight analyzer. A pulsed, low-energy (~18 eV) electron flood was then used to neutralize sample charging (the current was maintained

Rapid Communications in Mass Spectrometry

below ~20 μA maximum to avoid sample damage). The cycle time from starting a shot of the primary ion to the detection of secondary ions was 100 μs.

Negative secondary ion mass spectra were collected at three spots over an area of 500 μm × 500 μm with a pixel density of 128 × 128 on each of the PMMA samples for investigation of degrees of cross-linking on PMMA surfaces. A depth profile was obtained on a pristine and each of the 10-s, 100-s and 500-s HHIC-treated PMMA samples, by sputtering the surface in an area of 400 μm × 400 μm with a 10 keV C_{60}^+ ion beam (the target current was ~0.2 nA) for 1 s followed by analyzing the surface by collecting negative secondary ion mass spectra using the Bi_3^+ primary ion beam over an area of 200 μm × 200 μm within the sputtered area. The craters generated as a result of the depth profiling were examined using the profilometer, from which the measured depths were used to calibrate sputter depth. The negative secondary ion mass spectra were preliminarily calibrated using H^- and C^-. In order to establish a more accurate mass scale[38] for PMMA, the spectra were calibrated using the known CH^- and C_4H^- ions, and the characteristic PMMA ion, $C_4H_5O_2^-$. In the case that a more precise mass-to-charge ratio (*m/z*) was required to identify a peak, the mass scale was recalibrated using two known peaks, with one at a lower and the other at a higher *m/z* than the unknown peak. The mass resolutions for C_2H^- and C_6H^- were 2800 and 4400, respectively. Poisson-correction was applied for the dead time effect of the detecting system to correct the ion intensities.[39]

RESULTS AND DISCUSSION

Figure 1 shows an illustration of the negative ion fragmentation pattern of PMMA and a negative secondary ion mass spectrum obtained on the control (a pristine PMMA film spin-coated on a Si substrate). The most abundant fragment ion is $C_4H_5O_2^-$ (*m/z* 85), which is the monomer with the removal of the methyl group (CH_3) from the ether linkage (H_3C-O-C). As shown in the fragmentation pattern in Fig. 1, other ions at *m/z* 31, 55, 71, 141 and 185 are assigned to CH_3O^-, $C_3H_3O^-$, $C_3H_3O_2^-$, $C_8H_{13}O_2^-$ and $C_9H_{13}O_4^-$, respectively. Also seen in the spectrum are C_2HO^- (*m/z* 41) and CHO_2^- (*m/z* 45), which are less characteristic because they are also commonly seen for a wide variety of oxygen-containing organic molecules. The negative hydrocarbon ions C_2H^- (*m/z* 25) and C_4H^- (*m/z* 49) are ubiquitous for any surface containing hydrocarbons.

We have verified using atomic force microscopy (not shown) that there were no detectable changes in the surface morphology between the pristine and cross-linked PMMA films, while the chemical stability (i.e., resistance to solvent attack) of the cross-linked films was greatly enhanced. The HHIC technique has proven effective in cross-linking other organic molecular and polymer films with enhanced chemical stability and increased Young's modulus.[16,18] X-ray photoemission spectroscopy revealed that poly(acrylic acid) and poly(vinyl acetate) films cross-linked using the HHIC technique showed excellent retention of their functionalities.[16,17] Therefore, we concentrated on using TOF-SIMS to develop an analytical approach to assessing the degree and depth of cross-linking in PMMA films subjected to the HHIC treatment.

Figure 2 shows the negative secondary ion mass spectra for the control and the three PMMA samples subjected to HHIC treatment for 10, 100 and 500 s. There are abundant CN^- (*m/z* 26), C_3N^- (*m/z* 50) and $C_2N_3^-$ (*m/z* 66) ions upon HHIC treatment, which are probably caused by the residual nitrogen gas in the reactor. Also attributed to contamination in the reactor is the SO_4H^- (*m/z* 97) ion detected on the HHIC-treated samples. The intensities of the PMMA ions (e.g., $C_3H_3O^-$ and $C_4H_5O_2^-$) decreased drastically with increased HHIC treatment time. The observed decrease in ion intensities of the PMMA ions is a reflection that the cross-linked PMMA molecules no longer contribute to generating those ions.

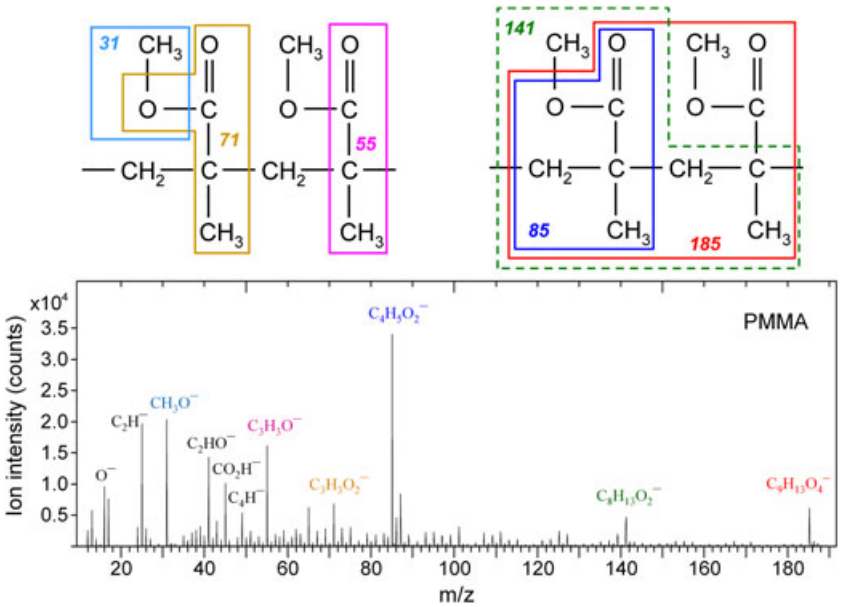

Figure 1. An illustration of the fragmentation pattern of PMMA showing the characteristic ion species and a negative secondary ion mass spectrum obtained on a PMMA film deposited on a Si wafer.

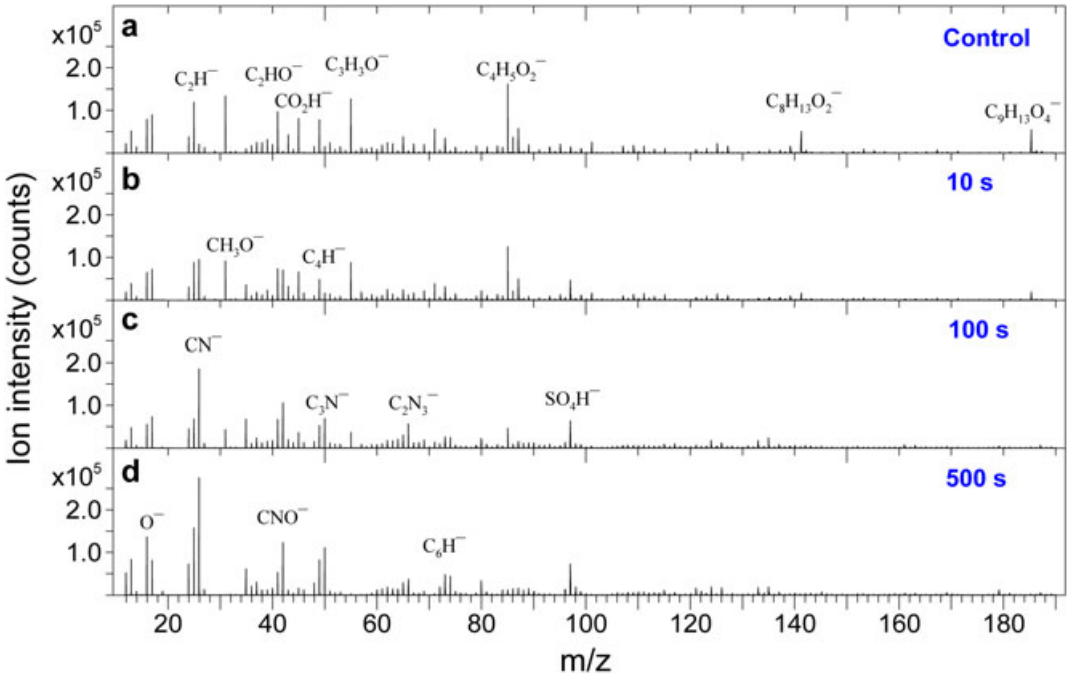

Figure 2. Negative secondary ion mass spectra obtained on (a) a pristine and three HHIC-treated PMMA for (b) 10, (c) 100 and (d) 500 s.

It is likely that, when all the contributing moieties in PMMA molecules are used up in cross-linking, the $C_4H_5O_2^-$ ions will vanish. Nevertheless, the altered polymer film may still be further cross-linked so long as C–H bonds are present. It is clear that when the degree of cross-linking of the PMMA film is small, the $C_4H_5O_2^-$ ion serves as a sensitive measure of cross-linking as long as monomers remain. For cross-linking beyond the point when no monomers are available, we need to look for other species to gauge the degree of cross-linking.

As shown in Fig. 2, increases in the intensities of C_4H^- and C_6H^- are clear for the 500-s treated PMMA sample in comparison with the control, while for the 10- and 100-s treated ones, the intensity increase is less obvious. Although not visible in Fig. 2, the C_8H^- and $C_{10}H^-$ intensities for the cross-linked PMMA films also were found to increase with increased HHIC treatment time. Intrigued by these observations, we examined the relationships between the intensities of the $C_{2n}H^-$ ions. The intensity ratio between C_6H^- and C_4H^- (hereafter denoted as ρ) for the PMMA films increased with increasing HHIC treatment time. We also found that, compared with other intensity ratios between the $C_{2n}H^-$ ions, ρ showed the largest variations as a function of HHIC treatment time. In fact, as demonstrated in a recent report, ρ is a convenient parameter to assess the carbon "density" of a polymer, although other ratios also work.[34] The cross-linking of PMMA induced by the HHIC treatment is a process of converting C–H bonds into C–C bonds, resulting in increases in carbon "density". Therefore, we propose to use ρ to assess degrees of cross-linking of the PMMA films. In this case, the PMMA ions (e.g., $C_4H_5O_2^-$), which are obviously a measure for degrees of cross-linking of the polymer, serve to validate our proposed ρ approach.

We select the most abundant ion $C_4H_5O_2^-$, normalized to C_4H^-, to represent PMMA. As shown in Fig. 3, the normalized $C_4H_5O_2^-$ intensity decreases rather quickly, from 5.9 for the control to 4.4, 0.8 and <0.1 upon HHIC treatment for 10, 100 and 500 s, respectively. This is a reflection that the PMMA molecules are cross-linked so that the amount of the contributing PMMA moiety usable for generation of the characteristic species is reduced. We verified that when the $C_4H_5O_2^-$ intensities are normalized to the total ion intensity, they still show the same trend as those normalized by the C_4H^- intensity, as shown in Fig. 3. On the other hand, ρ increases with increasing HHIC treatment time. Specifically, ρ for the control is 32.2 ± 0.3%, while for the 10-s, 100-s and

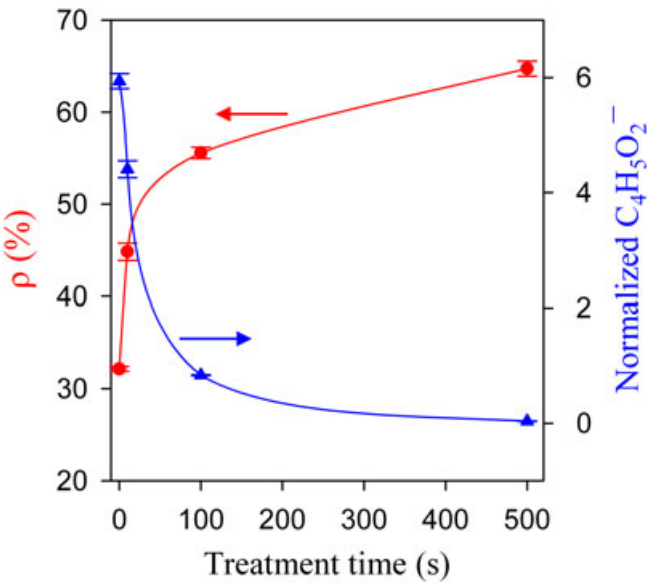

Figure 3. Ion intensities of C_6H^- (ρ) (filled circles) and $C_4H_5O_2^-$ (filled triangles) normalized to C_4H^-as a function of HHIC treatment time.

Rapid Communications in Mass Spectrometry

500-s HHIC-treated samples it increases to 44.8 ± 0.9%, 55.6 ± 0.6% and 64.7 ± 0.8%, respectively. Those numbers can be used as a new scale for estimating degrees of cross-linking with ρ = 32% for the control and ρ = 65% corresponding to heavily cross-linked PMMA. Therefore, ρ may serve as a TOF-SIMS criterion leading to the quantification of the degree of cross-linking of cross-linked PMMA films. We verified that this analytical approach was applicable in other materials, such as dotriacontane ($C_{32}H_{64}$) monolayers and poly(acrylic acid) films,[16] which were cross-linked using the HHIC technique. They showed similar trends to those that were seen in PMMA.

It will be interesting to compare this new scale with other scales of degree of cross-linking[19] used in some of the conventional methods, such as increased modulus and hardness,[18,40] which is the objective of ongoing research. This TOF-SIMS approach is especially promising in assessing degrees of cross-linking of ultra-thin films where use of other existing techniques is extremely difficult, if not impossible. We point out that C_8H^- and $C_{10}H^-$ serve a similar purpose to C_6H^-, although their intensities are much lower than that of C_6H^- and they interfere with the PMMA ions $C_5H_5O_2^-$ and $C_7H_5O_2^-$, respectively, when the degree of cross-linking is minimal.

The interpretation of the detection of linear hydrocarbon chains $C_{2n}H^-$ by TOF-SIMS is that these ions are not structural entities in the polymer film; they ought to form by the combination of multiple atoms/ions of carbon and a single atom/ion of hydrogen, which are generated due to the primary ion beam bombardment.[34] Their structures can be explained by carbons connected via alternating single and triple bonds with one end of the carbon chain terminated by a hydrogen atom and the other being a carbon radical displaying a negative charge.[41–44]

The experimental observations that ρ is capable of assessing degrees of cross-linking of PMMA implies that the $C_{2n}H^-$ ions carry information on its chemical structure. The HHIC treatment is basically a process of removing hydrogen atoms from C–H bonds, in which two C–H bonds, each in two hydrocarbon chains, are converted into a C–C bond (so that the two hydrocarbon chains are cross-linked). With increased degrees of cross-linking, more C–H bonds would be converted into C–C bonds, resulting in increased ρ, as shown in Fig. 3. In fact, it has been demonstrated that ρ has fixed values of 20%, 23%, 27% and 53% for PE, PP, PIP and PS, respectively.[34] Among these polymers, PE has a straight hydrocarbon chain without any branches, in which every carbon atom is bonded to two carbon and two hydrogen atoms, thus having the highest number of hydrogen atoms, or the lowest carbon "density".[34] In contrast, the carbon "density" in PS is the highest among the four samples. This is consistent with the observed variations of ρ in the HHIC-treated PMMA samples as cross-linking is basically a process of removing hydrogen from the polymer, which is equivalent to an increase in carbon "density". These experimental observations led us to conclude that PMMA with a higher carbon "density", i.e., a higher degree of cross-linking, prefers formation of

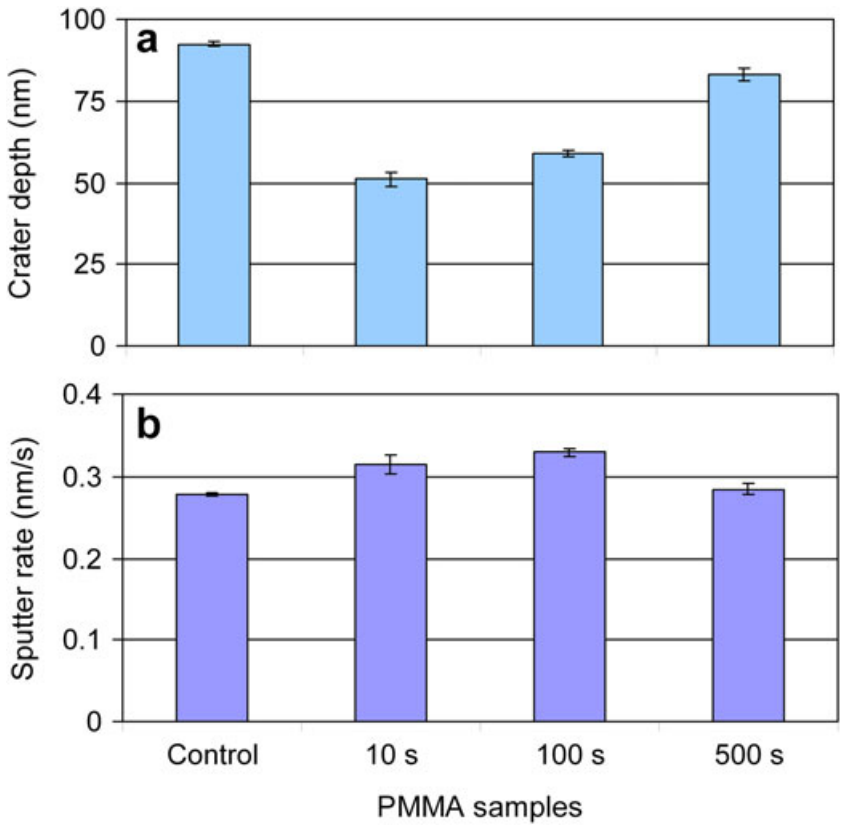

Figure 4. The crater depth (a) and sputter rate (b) for the control and HHIC-treated PMMA samples for 10, 100 and 500 s upon depth profiling using a 10 keV C_{60}^+ sputter beam.

larger carbon clusters, thus yielding a larger value of ρ. Therefore, ρ serves as a new scale enabling us to assess the degree of cross-linking of PMMA.

Since adventitious hydrocarbons exist on any surface exposed to air, it is important to clarify whether this ubiquitous contamination affects the observed $C_{2n}H^-$ intensities for PMMA. As shown above, PMMA and the four polymers examined in a previous report[34] are characterized by a different but fixed value of ρ. This implies that ρ is characteristic to the chemical structure of a polymer, rather than a reflection of the ubiquitous adventitious hydrocarbons.

With ρ being capable of quantifying the degree of cross-linking on the surface of the cross-linked PMMA films by the surface-sensitive cross-linking HHIC technique, it is also important to assess its variations as a function of depth. TOF-SIMS is useful for this depth profiling task by repeating the cycle of using a C_{60}^+ sputter beam to remove a controllable amount of substance followed by analyzing the newly generated surface using the Bi_3^+ primary ion beam. In the sputter process, the sputter time was used to control the amount of substance to be removed. We used a profilometer to measure the depth of the crater generated as a result of the depth profiling, and this allowed us to calibrate the sputter depth. The crater depths and the sputter rates for the control and the HHIC-treated PMMA films for 10, 100 and 500 s are shown in Figs. 4(a) and 4(b), respectively. The sputter rates for the four samples are estimated to be approximately 0.30 nm/s with a standard deviation of 10%.

Figure 5(a) shows the results of depth profiling ρ for the three HHIC-treated PMMA films and the control, and these offer a clear view to both degrees and depths of cross-linking for the cross-linked PMMA films. We first look at the most important observations on the three HHIC-treated PMMA films. It is clear that ρ decreases with different characteristics as a function of HHIC treatment time; that is, the longer the HHIC treatment time the higher the value of ρ and the deeper the cross-linking penetrates into the film. It is interesting to note that ρ converges to ~40% at a depth dependent on the HHIC treatment time and plateaus thereafter, which is a measure of where cross-linking penetrates. Because the decrease in ρ as a function of depth for the three HHIC-treated PMMA films appears to be exponential, we tried to determine the cross-linking depth by curve fitting a depth profile of ρ to an exponential decay $\rho(z) = \rho_{min} + (\rho_{max} - \rho_{min})e^{-kz}$, where k is the decay constant, ρ_{max} the maximum ρ (i.e., at the film surface) and ρ_{min} the minimum ρ (i.e., after the cross-linked portion of the PMMA film is removed by the C_{60}^+ sputter beam). The estimated values of k for the HHIC-treated PMMA films for 10, 100 and 500 s are 0.711, 0.153 and 0.059 nm^{-1}, respectively.

With the decay constant now known, we can evaluate from the exponential decay equation the depth corresponding to any value of ρ. For example, the half depth, defined as the depth where ρ decreases to half of the maximum (with the minimum being offset), is $z_{1/2} = \ln(2)/k = 0.693/k$. The half depths for the HHIC-treated PMMA for 10, 100 and 500 s are determined to be 1, 5 and 12 nm, respectively. By defining the cross-linking depth as being the depth where ρ decreases to 10% of its maximum, $z_{1/10} = \ln(10)/k = 2.30/k$, we estimate that the cross-linking depths for the PMMA films treated by HHIC for 10, 100 and 500 s are 3, 15 and 39 nm, respectively.

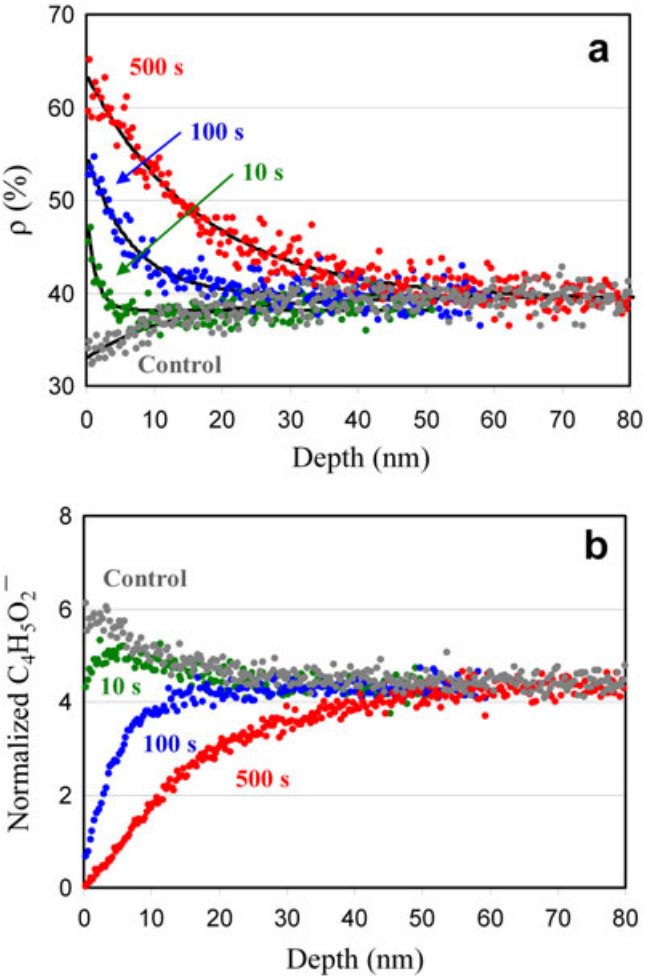

Figure 5. Depth profiles of ion intensity ratio to C_4H^- of (a) C_6H^- (ρ) and (b) $C_4H_5O_2^-$ for the control and the HHIC treated PMMA films for 10, 100 and 500 s.

It is thus clear that cross-linked PMMA molecules even within a depth of a mere several nanometers can be easily profiled using TOF-SIMS.

The depth profile for the control shows that ρ at the surface is ~32%, while this increases to ~40% at a depth of ~30 nm and then plateaus. This depth profile for the PMMA control is important in revealing some aspects of depth profiling in our experiment. It is clear that the sputtering C_{60}^+ beam induces alterations in the polymer so that its ρ value gets increasingly larger when depth profiling into the film. Nevertheless, the increase in ρ induced by C_{60}^+ sputtering does not exceed that induced by cross-linking the polymer film using the HHIC technique. Our experiment has thus proven that C_{60}^+ is suitable for depth profiling the cross-linking depth of the PMMA films.

Figure 5(b) shows the depth profiles of the PMMA ion $C_4H_5O_2^-$, which serve to verify the cross-linking of PMMA and confirm the recovery of the PMMA species after the cross-linked portion is removed by C_{60}^+ sputtering. The depth profile of the control shows that the normalized ion intensity of the PMMA species (~6 at the surface) decreases while the polymer film is being depth profiled and converges to ~4 at a depth of ~30 nm, suggesting that the

polymer film is altered upon the C_{60}^+ sputtering. This behavior has been observed on many organic films, and it is attributable to damages left on the sputtered organic film surface.[45,46]

The maximum damage level caused by C_{60}^+ sputtering is characterized by a normalized $C_4H_5O_2^-$ of ~4 (Fig. 5(b)) and a ρ value of ~40% (Fig. 5(a)) when the films were profiled well into the control. However, alterations in ion intensities induced by the sputtering, although existing, are far from invalidating depth profiling of the cross-linked PMMA. For example, even for the least cross-linked (i.e., the 10-s HHIC treated) sample, its depth profiles are clearly distinguishable from those of the control. Therefore, the depth profiles in Fig. 5 clarify that the C_{60}^+ sputtering worked in depth profiling the degrees of cross-linking of PMMA films because the damage levels did not significantly affect the results. This ion beam, however, will not work on other polymers such as PE, PP and PS, which are easily damaged by C_{60}^+ sputtering. Therefore, it is expected that depth profiling the degree of cross-linking of these polymers will require (a) other sputter ion sources, which can be devised with a low energy Cs^+ beam[28,47] or gas cluster ion beams such as large Ar clusters,[48] as well as (b) introduction of nitric oxide gas to the analysis chamber as a radical scavenger to reduce damage caused by C_{60}^+ sputtering.[29,49]

CONCLUSIONS

We have demonstrated that the intensity ratio of the C_6H^- and C_4H^- ions detected in TOF-SIMS, denoted as ρ, provides a unique and simple means to assess degrees of cross-linking of spin-coated PMMA films cross-linked by the HHIC technique. With the un-crosslinked PMMA having a ρ value of 32% when using a 25 keV Bi_3^+ analysis ion beam, this parameter measured at the PMMA film surfaces increased to 45%, 56% and 65% when subjected to HHIC treatment for 10, 100 and 500 s, respectively. With a 10 keV C_{60}^+ sputter ion beam, we obtained depth profiles of ρ resembling exponential decays, from which the cross-linking depths were estimated to be 3, 15 and 39 nm for these three cross-linked PMMA films, respectively. Our TOF-SIMS results thus verified that the HHIC technique is able to control the depth of cross-linking on nanometer scales. The TOF-SIMS approach that we have developed will enable researchers in polymer science and engineering to assess degrees of cross-linking and depths for either ultra-thin polymer films or ultra-thin portions of polymer films that are cross-linked.

Acknowledgements

This work was supported by a University Partnership Committee Funded Research contract from Xerox Research Centre of Canada and a Collaborative Research & Development grant from the Natural Sciences and Engineering Research Council of Canada (CRDPJ 414321-11). The authors greatly acknowledge Drs Igor Bello and Thomas Trebicky for building the HHIC reactor system at Surface Sciecne Western.

REFERENCES

[1] W. W. Flack, D. Soong, A. Bell, D. Hess. A mathematical model for spin coating polymer resists. *J. Appl. Phys.* **1984**, *56*, 1199.
[2] K. Norrman, A. Ghanbari-Siahkali, N. B. Larsen. Studies of spin-coated polymer films. *Annu. Rep. Prog. Chem., Sect. C* **2005**, *101*, 174.
[3] D. T. W. Toolan, J. R. Howse. Development of *in situ* studies of spin coated polymer films. *J. Mater. Chem. C* **2013**, *1*, 603.
[4] C. V. Bonduelle,W. M. Lau, E. R. Gillies. Preparation of protein- and cell-resistant surfaces by hyperthermal hydrogen induced cross-linking of poly(ethylene oxide). *ACS Appl. Mater. Interfaces* **2011**, *3*, 1740.
[5] S. Karamdoust, B. Y. Yu, C. V. Bonduelle, Y. Liu, G. Davidson, G. Stojcevic, J. Yang, W. M. Lau, E. R. Gillies. Preparation of antibacterial surfaces by hyperthermal hydrogen induced cross-linking of polymer thin films. *J. Mater. Chem.* **2012**, *22*, 4881.
[6] K. Haupt, K. Mosbach. Molecularly imprinted polymers and their use in biomimetic sensors. *Chem. Rev.* **2000**, *100*, 2495.
[7] C. J. Drury, C. M. J. Mutsaers, C. M. Hart, M. Matters, D. M. de Leeuw. Low-cost all-polymer integrated circuits. *Appl. Phys. Lett.* **1998**, *73*, 108.
[8] C. R. Newman, C. D. Frisbie, D. A. da Silva Filho, J.-L. Bredas, P. C. Ewbank, K. R. Mann. Introduction to organic thin film transistors and design of n-channel organic semiconductors. *Chem. Mater.* **2004**, *16*, 4436.
[9] S. R. Forrest. The path to ubiquitous and low-cost organic electronic appliances on plastic. *Nature* **2004**, *428*, 911.
[10] A. Facchetti, M.-H. Yoon, T. J. Marks. Gate dielectrics for organic field-effect transistors: New opportunities for organic electronics. *Adv. Mater.* **2005**, *17*, 1705.
[11] H. Ma, H. L. Yip, F. Huang, A. K. Y. Jen. Interface engineering for organic electronics. *Adv. Funct. Mater.* **2010**, *20*, 1371.
[12] H. Klauk. Organic thin-film transistors. *Chem. Soc. Rev.* **2010**, *39*, 2643.
[13] G.A. Senich, R.E. Florin. Radiation curing of coatings. *J. Macromol. Sci-Rev. Macromol. Chem. Phys. C* **1984**, *24*, 239.
[14] J. M. Spruell, M. Wolffs, F. A. Leibfarth, B. C. Stahl, J. H. Heo, L. A. Connal, J. Hu, C. J. Hawker. Reactive, multifunctional polymer films through thermal cross-linking of orthogonal click groups. *J. Am. Chem. Soc.* **2011**, *133*, 16698.
[15] S. Edmondson, V. L. Osborne, W. T. S. Huck. Polymer brushes via surface-initiated polymerizations. *Chem. Soc. Rev.* **2004**, *33*, 14.
[16] T. Trebicky, P. Crewdson, M. Paliy, I. Bello, H.-Y. Nie, Z. Zheng, X. L. Fan, J. Yang, E. R. Gillies, C. Y. Tang, H. Liu, K. W. Wong, W. M. Lau. Cleaving C–H bonds with hyperthermal H2: facile chemistry to cross-link organic molecules under low chemical- and energy-loads. *Green Chem.* **2014**, *16*, 1316.
[17] D. B. Thompson,T. Trebicky, P. Crewdson, M. J. McEachran, G. Stojcevic, G. Arsenault, W. M. Lau, E. R. Gillies. Functional polymer laminates from hyperthermal hydrogen induced cross-linking. *Langmuir* **2011**, *27*, 14820.
[18] Y. Liu, D.-Q. Yang, H.-Y. Nie, W. M. Lau, J. Yang. Study of a hydrogen-bombardment process for molecular cross-linking within thin films. *J. Chem. Phys.* **2011**, *134*, 074704.
[19] C. Hirschl, M. Biebl–Rydlo, M. DeBiasio, W. Mühleisen, L. Neumaier, W. Scherf, G. Oreski, G. Eder, B. Chernev, W. Schwab, M. Kraft. Determining the degree of crosslinking of ethylene vinyl acetate photovoltaic module encapsulants - A comparative study. *Solar Ener. Mater. Solar Cells* **2013**, *116*, 203.
[20] A. Benninghoven. Chemical analysis of inorganic and organic surfaces and thin films by static time-of-flight

secondary ion mass spectrometry (TOF-SIMS). *Angew. Chem. Int. Ed. Engl.* **1994**, *33*, 1023.
[21] J. S. Fletcher, N. P. Lockyer, S. Vaidyanathan, J. C. Vickerman. TOF-SIMS 3D biomolecular imaging of *Xenopus laevis* oocytes using buckminsterfullerene (C_{60}) primary ions. *Anal. Chem.* **2007**, *79*, 2199.
[22] A. M. Belu, M. C. Davies, J. M. Newton, N. Patel. TOF-SIMS characterization and imaging of controlled-release drug delivery systems. *Anal. Chem.* **2000**, *72*, 5625.
[23] J. H. Wandass, J. A. Gardella. Secondary ion mass spectrometry of monomolecular layers of fatty acids prepared by Langmuir-Blodgett techniques. *J. Am. Chem. Soc.* **1985**, *107*, 6192.
[24] A. Chilkoti, G. P. Lopez, B. D. Ratner, M. J. Hearn, D. Briggs. Analysis of polymer surfaces by SIMS. 16. Investigation of surface cross-linking in polymer gels of 2-hydroxyethyl methacrylate. *Macromolecules* **1993**, *26*, 4825.
[25] H.-Y. Nie. Revealing different bonding modes of self-assembled octadecylphosphonic acid monolayers on oxides by time-of-flight secondary ion mass spectrometry: Silicon vs aluminum. *Anal. Chem.* **2010**, *82*, 3371-3376.
[26] A. G. Shard, P. J. Brewer, F. M. Green, I. S. Gilmore. Measurement of sputtering yields and damage in C_{60} SIMS depth profiling of model organic materials. *Surf. Interface Anal.* **2007**; *39*: 294.
[27] L. L. Zheng, A. Wucher, N. Winograd. Depth resolution during C_{60}^+ profiling of multilayer molecular films. *Anal. Chem.* **2008**, *80*, 7363.
[28] C. M. Mahoney. Cluster secondary ion mass spectrometry of polymers and related materials. *Mass Spectrom. Rev.* **2010**, *29*, 247.
[29] R. Havelund, A. Licciardello, J. Bailey, N. Tuccitto, D. Sapuppo, I. S. Gilmore, J. S. Sharp, J. L. S. Lee, T. Mouhib, A. Delcorte. Improving secondary ion mass spectrometry C_{60}^{n+} sputter depth profiling of challenging polymers with nitric oxide gas dosing. *Anal. Chem.* **2013**, *85*, 5064.
[30] R. J. Paruch, B. J. Garrison, Z. Postawa. Computed molecular depth profile for C_{60} bombardment of a molecular solid. *Anal. Chem.* **2013**, *85*, 11628.
[31] D. Briggs. Analysis of polymer surfaces by SIMS. 14. Aliphatic hydrocarbons revisited. *Surf. Interface Anal.* **1990**, *15*, 734.
[32] C.-M. Chan, L.-T. Weng, Y.-T. R. Lau. Polymer surface structures determined using ToF-SIMS. *Rev. Anal. Chem.* **2014**, *33*, 11.
[33] S. Ligot, E. Bousser, D. Cossement, J. Klemberg-Sapieha, P. Viville, P. Dubois, R. Snyders. Correlation between mechanical properties and cross-linking degree of ethyl lactate plasma polymer films. *Plasma Process. Polym.* **2015**, *12*, 508.
[34] H.-Y. Nie. Negative hydrocarbon species $C_{2n}H^-$: How useful can they be? *J. Vac. Sci. Technol. B* **2016**, *34*, 030603.
[35] Z. J. Jia, Z. Y. Wang, C. L. Xu, J. Liang, B. Q. Wei, D. H. Wu, S. W. Zhu. Study on poly(methyl methacrylate)/carbon nanotube composites. *Mater. Sci. Eng.: A* **1999**, *271*, 395.
[36] S. Gross, D. Camozzo V. Di Noto, L. Armelao, E. Tondello. PMMA: A key macromolecular component for dielectric low-κ hybrid inorganic–organic polymer films. *Eur. Polym. J.* **2007**, *43*, 673.
[37] M. Na, S.-W. Rhee. Electronic characterization of Al/PMMA[poly(methyl methacrylate)]/p-Si and Al/CEP(cyanoethyl pullulan)/p-Si structures. *Org. Electron.* **2006**, *7*, 205.
[38] F. M. Green, I. S. Gilmore, M. P. Seah. TOF-SIMS: Accurate mass scale calibration. *J. Am. Soc. Mass Spectrom.* **2006**, *17*, 514.
[39] T. Stephan, J. Zehnpfenning, A. Benninghoven. Correction of dead time effects in time-of-flight mass spectrometry. *J. Vac. Sci. Technol. A* **1994**, *12*, 405.
[40] L. A. Pruitt. Deformation, yielding, fracture and fatigue behavior of conventional and highly cross-linked ultra high molecular weight polyethylene. *Biomater.* **2005**, *26*, 905.
[41] Y.-L. Sun, W.-J. Huang, S.-H. Lee. Formation of polyynes C_4H_2, C_6H_2, C_8H_2, and $C_{10}H_2$ from reactions of C_2H, C_4H, C_6H, and C_8H radicals with C_2H_2. *J. Chem. Phys. Lett.* **2015**, *6*, 4117.
[42] S. J. Blanksby, A. M. McAnoy, S. Dua, J. H. Bowie. Cumulenic and heterocumulenic anions: Potential interstellar species? *Mon. Not. R. Astron. Soc.* **2001**, *328*, 89.
[43] L. Pan, B. K. Rao, A. K. Gupta, G. P. Das, P. Ayyub. H-substituted anionic carbon clusters C_nH^- ($n \leq 10$): Density functional studies and experimental observations. *J. Chem. Phys.* **2003**, *119*, 7705.
[44] M. Fehér and J. P. Maier. The geometric and electronic structures of C_6H and its ions. *Chem. Phys. Lett.* **1994**, *227*, 371.
[45] J. Cheng, A. Wucher, N. Winograd. Molecular depth profiling with cluster ion beams. *J. Phys. Chem. B* **2006**, *110*, 8329.
[46] E. A. Jones, N. P. Lockyer, J. C. Vickerman. Mass spectral analysis and imaging of tissue by ToF-SIMS – The role of buckminsterfullerene, C_{60}^+, primary ions. *Int. J. Mass Spectrom.* **2007**, *260*, 146.
[47] N. Mine, B. Douhard, J. Brison, L. Houssiau. Molecular depth-profiling of polycarbonate with low-energy Cs^+ ions. *Rapid Commun. Mass Spectrom.* **2007**, *21*, 2680.
[48] S. Ninomiya, K. Ichiki, H. Yamada, Y. Nakata, T. Seki, T. Aoki, J. Matsuo. Precise and fast secondary ion mass spectrometry depth profiling of polymer materials with large Ar cluster ion beams. *Rapid Commun. Mass Spectrom.* **2009**, *23*, 1601.
[49] G. Zappalà, V. Motta, N. Tuccitto, S. Vitale, A. Torrisi, A. Licciardello. Nitric oxide assisted C_{60} secondary ion mass spectrometry for molecular depth profiling of polyelectrolyte multilayers. *Rapid Commun. Mass. Spectrom.* **2015**, *29*, 2204.

